The energy dependence of secondary emission based on the range-energy retardation power formula

1979 J. Phys. D: Appl. Phys. 12 619

(http://iopscience.iop.org/0022-3727/12/4/019)

J. Phys. D: Appl. Phys., Vol. 12, 1979. Printed in Great Britain

The energy dependence of secondary emission based on the range–energy retardation power formula

Susumu Ono and Koichi Kanaya
Department of Electrical Engineering, Kogakuin University, 1-24-2 Nishi-Shinjuku, Shinjuku-ku, Tokyo, Japan 160

Received 11 September 1978

Abstract. Based on the energy retardation power formula concerning the penetration and the energy loss of an electron probe into solid targets, the secondary electron emission yield δ due both to primary and back-scattered electrons is derived as functions of three parameters such as atomic number Z, first ionisation energy I and back-scattering coefficient r, which are found to be in good accordance with the results obtained experimentally.

Notable in such theoretical procedures are the maximum yield δ_m and the primary energy E_m, giving

$$\delta_m = 0{\cdot}12\, Z^{1/15}\, I^{4/5}\, (1 + 1{\cdot}26\, r)$$

for

$$E_m = 57{\cdot}9\, Z^{1/15}\, I^{4/5}\, (1 + 5\, r^2)^{4/5}\ (\text{eV})$$

which substantially agree with the miscellaneous experiments of many authors.

The energy dependence of the yield–energy distributions, the yield of thin films and the lateral distribution of secondary yield at the distance from the centre of the beam are given as functions of the back-scattering coefficient and the primary energy.

1. Introduction

Many attempts have been made to explain secondary electron emission induced by electron bombardment qualitatively and quantitatively since the work of Austin and Starke (1902). Recently, a considerable interest has arisen in the use of secondary electron emission from a solid target by the bombardment of a finely focused and highly accelerated beam of electrons as in scanning electron microscopes. The quantitative analysis of secondary electron images in scanning electron microscopes requires the exact values of yield, the escape depth of secondary electrons, and the contribution of back-scattered electrons within a solid target.

Based on the assumption of two mechanisms in the secondary electron emission process (the production and escape mechanisms of secondary electrons), there have been some theories of the secondary emission, such as a free-electron theory of Baroody (1950), cascade theory of Wolff (1954), and quantum theory of the production of secondaries (Fröhlich 1932, Wooldridge 1939, Dekker and van der Ziel 1952, Marshall 1952, van der Ziel 1953, Baroody 1953, 1956). In addition, the semi-empirical theories based on the electron range–energy power-law (the Thomson–Whiddington law) have been presented

0022-3727/79/040619+14 $01.00

by Salow (1940), Bruining (1954), Jonker (1952, 1954), Lye and Dekker (1957), and Dekker (1958).

In the recent work, Kanaya and Kawakatsu (1972) and Dionne (1973, 1975) have developed the theory of secondaries by the generalised power law concerning the energy loss of electrons penetrating into a solid target making use of range measurements by Glendenin (1948), Katz and Penfold (1952), Lane and Zaffarano (1954), Young (1956), Holliday and Sternglass (1959), and by Cosslett and Thomas (1964).

In this paper, an attempt is made to present a sufficient solution of the secondary electron yield of metals and semiconductor compounds except insulators, by applying the free-electron scattering theory to the absorption of secondary electrons generated within a solid target. For insulators, Kanaya *et al* (1978) have presented a sufficient solution of the high yield and an explanation of the different yield appearing in integral multiples, combining the free-electron scattering theory with the plasmon theory.

By using the potential function of the power and exponential forms as a function of a modified screened atomic radius for electron scattering (Kanaya and Ono 1976), the range–energy relationship of $R=(E_0/E_R)^{1+1/n}/c_0$, with an incident energy E_0 of between 1 keV and 1 MeV, is used as a fundamental equation, where n indicates the degree of screening (n goes from 1 to ∞ as the accelerating voltage decreases), E_R is the Rydberg energy and c_0 the range–energy coefficient of the primary beam.

The purely classical empirical theory (Bruining 1954, Jonker 1952, 1954, Lye and Dekker 1957, Kanaya and Kawakatsu 1972) is developed by the power law concerning the energy loss. Also, by using the absorption law of Lenard type and the assumption that the distribution of secondary electrons with energies below 50 eV produced by primary electrons within the target is isotropic, the universal yield–energy curve is deduced. It is shown that the absorption coefficient of secondary electrons involved in the Lenard law relates with the suitably averaged ionisation loss, since the energy of secondary electrons produced by the first collision of primary electrons with the target is very small, i.e. $E_s=100$–200 eV (Rauth and Simpson 1964).

Since the resulting maximum yield δ_m and the energy E_m mainly depend on the range–energy coefficient of the primary beam c_0 and the absorption coefficient α, these can be given as functions of ionisation energy I, back-scattering coefficient r and the atomic number Z.

2. Absorption coefficient α and escape depth x_α

The absorption coefficient α of secondary electrons generated within the solid target is a most significant factor in quantitative evaluation of the maximum yield δ_m which is, in practice, measured with its corresponding incident energy E_m.

Suppose that the secondary electrons are distributed following the Lenard (1918) law after their dislodgement and satisfy the special case $n=4$ of the power law in the first collision.

Since their energy of most probable ionisation loss in the first collision is very low ($E_s=100$–200 eV, Rauth and Simpson 1964) compared with the primary energy $E_0 \geqslant 5$ keV, the transmission fraction of secondaries is given by

$$i_s/i_0=\exp(-N\sigma_i x)=\exp(-\alpha x) \tag{1}$$

where i_s is the secondary emission current, i_0 the primary beam current, N the number of atoms per unit volume, and σ_i is the total scattering cross-section due to the loss of secondary electrons.

Then, the total cross-section σ_i (for secondary emission) (Kanaya and Ono 1976) is given by

$$\sigma_i = \lambda_\infty{}^2 4\pi Z a^2 (E_R/E_s) \ln\left(\frac{4E_s}{I}\right) \tag{2}$$

where $\lambda_\infty{}^2$ is the constant determined empirically, $a = 0{\cdot}77 a_H Z^{-1/6}$ the screened atomic radius, a_H the Bohr radius of hydrogen, and $n = \infty$ is assumed because the energy of secondary electrons is very low. The ionisation energy E_s is ranged between 92 and 235 eV for Al, Cu, Si and Au (Rauth and Simpson 1964), and it can be approximated as

$$E_s = n_s I \tag{3}$$

where I is the first ionisation energy and n_s, the constant, is taken to be $n_s = 20$.

Accordingly, the most probable escape depth of secondary electrons x_α, in a similar manner to the diffusion model by Archard (1961), from $i_s/i_0 = 1/e$, is given by

$$x_\alpha = 1/\alpha = 2{\cdot}67\, A_0 I/\rho Z^{2/3}\ (\text{Å}) \tag{4}$$

where $\lambda_\infty{}^2 = 0{\cdot}1$ is used. A_0 the atomic weight and ρ the density. Figure 1 shows the escape depth of secondary electrons x_α as a function of atomic number Z, which is in good agreement with Seiler's (1967) data.

3. Secondary yield due to primary and back-scattered electrons

According to the elementary theory, the number of secondary electrons ejected from the target increase in proportion to the energy loss, they are isotropically distributed in the

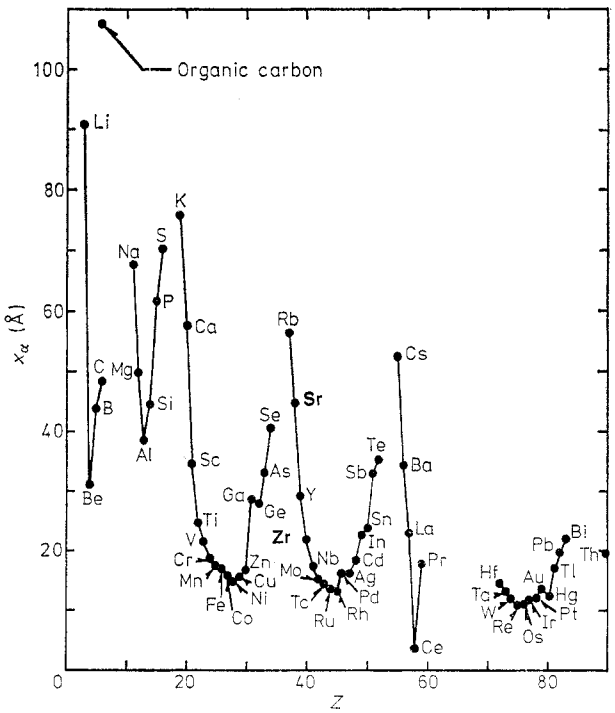

Figure 1. The escape depth of secondary electrons x_α as a function of atomic number Z. $x_\alpha = 2{\cdot}67\, A_0 I/\rho Z^{2/3}$ Å.

solid target, and are emitted from the surface following the absorption law of Lenard type after their dislodgement.

The analytical treatments, as well as Monte-Carlo calculations, are very useful to evaluate the secondary electron emission mechanisms from metals by electron beam bombardment, which have been developed by Jonker (1952, 1954) and Lye and Dekker (1957) and others, and Reimer (1968), Shimizu and Murata (1971), Shimizu (1974), Ganachaud and Cailler (1975a,b), Ganachaud (1977), and Pillon and Ganachaud (1977), respectively.

Suppose an incident electron beam falls perpendicularly on a solid target. The number of secondary electrons released is proportional to the electron energy loss dE/dx. They arrive at the surface by travelling a distance $l=x/\cos\theta$ through the material, and the secondary yield is given by Jonker (1952, 1954) and Kanaya and Kawakatsu (1972) as

$$\delta=\frac{K}{2}\int_0^R \frac{d(E/E_R)}{dx}\int_0^{\pi/2}\exp\left(-\frac{\alpha x}{\cos\theta}\right)\sin\theta\,d\theta\,dx \tag{5}$$

where K is the constant depending on the penetration of electrons.

By using the range–energy relationship and the resulting energy retardation formula (Kanaya and Ono 1976), the secondary yield due to primary electrons δ_p, can be given by

$$\delta_p=\frac{K}{2}\left(\frac{c_0}{\alpha}\right)^{n/(1+n)}\int_0^1 \frac{n}{1+n}A^{n/(1+n)}(1-y)^{-1/(1+n)}[\exp(-Ay)+AyE_i(-Ay)]\,dy \tag{6}$$

where

$$A=\alpha R=(\alpha/c_0)(E_0/E_R)^{1+1/n} \qquad \text{and} \qquad E_i(-x)=-\int_x^\infty \exp(-t)/t\,dt$$

is the exponential integral function.

Most incident electrons are scattered through small angles as they interact with atoms. As the electron penetration increases deeply, the primary beam spreads in a Gaussian manner, as shown in a previous paper of diffusion model (Kanaya and Ono 1978). Consideration of the back-scattered electrons becomes especially important because their maxima are ranged between 500 and 2000 eV. According to Kanter (1961) the back-scattered electrons from the interior of the material follow a cosine distribution. Therefore the rate of energy loss and the path lengths of back-scattered electrons in the region of secondary escape are large compared with those of the incoming primaries. Thus the secondary electron yield cannot be disregarded when the back-scattering coefficient η_B is relatively large.

Consider the production of secondary electrons by back-scattered electrons, from the generalised case of primary electrons, the secondary yield due to back-scattered electrons δ_B is given by

$$\delta_B=\eta_B\left(\frac{K}{2}\right)\left(\frac{c_0}{\alpha}\right)^{n/(1+n)}\int_0^{1/2}\left(\frac{2n}{1+n}\right)(1-y)^{(n-1)/(n+1)}$$
$$\times A^{n/(1+n)}[\exp(-Ay)+AyE_i(-Ay)]\,dy. \tag{7}$$

The total secondary yield δ is then considered to be the sum of the primary and back-scattered electrons:

$$\delta=\delta_p+\delta_B. \tag{8}$$

It can be simply expressed by

$$\delta/[(K/2)(c_0/\alpha)^{n/(1+n)}]=f_p(A)+\eta_B f_B(A) \tag{9}$$

in which $f_p(A)$ and $f_B(A)$ are the integrations in equations (6) and (7), respectively, and have maxima as shown in Kanaya *et al* (1978).

Accordingly, the value of total yield normalised by the maximum yield δ/δ_m can be obtained as a function of E/E_m:

$$\delta/\delta_m = [f_p(A)+\eta_B f_B(A)]/[f_p(A)+\eta_B f_B(A)]_{max} \tag{10}$$

for $E/E_m=(A/A_m)^{n/(1+n)}$. For the sake of simplicity for the calculation, it can be numerically approximated as

$$[f_p(A)+\eta_B f_B(A)]_{max}=0{\cdot}365\,(1+1{\cdot}26\,r) \tag{11}$$

and

$$A_m=(1+5r^2) \tag{12}$$

where the back-scattering coefficient $r=[\eta_B]_{y=1/2}$, where η_B is the back-scattering fraction with depth $y=x/R$, is used from the diffusion model (Kanaya and Ono 1978) as

$$r=\tfrac{1}{2}(1-\cos\theta_0) \tag{13}$$

with

$$\tan\theta_0=\frac{2{\cdot}2\gamma}{1+2\gamma-0{\cdot}21\gamma^2}$$

$$\gamma=\Omega(n-1)(Z+1)/[n(n+1)2^{1/n}]$$

$$\Omega=\tfrac{1}{3}\left(\int_0^{\pi/2}d\Omega+\frac{1}{2!}\int_{\pi/2}^{3\pi/4}d\Omega+\frac{1}{3!}\int_{\pi/2}^{5\pi/6}d\Omega\right)$$

$$d\Omega=\sin\theta\,d\theta/(1+\cos\theta)^{1+1/n}$$

which is very close with the empirical result by Weinryb and Philibert (1964).

Figure 2 represents the theoretical and experimental comparison of the universal yield–energy curve for the energy-dependent parameter n, where the upper limit of the curve corresponds to the light element of the target and lower limit to the heavy element, respectively, and the yield increases as the back-scattering coefficient η_B increases. The energy and back-scattering dependence of the universal yield–energy curves are in good agreement with the experiments of Si, Ni and Mo.

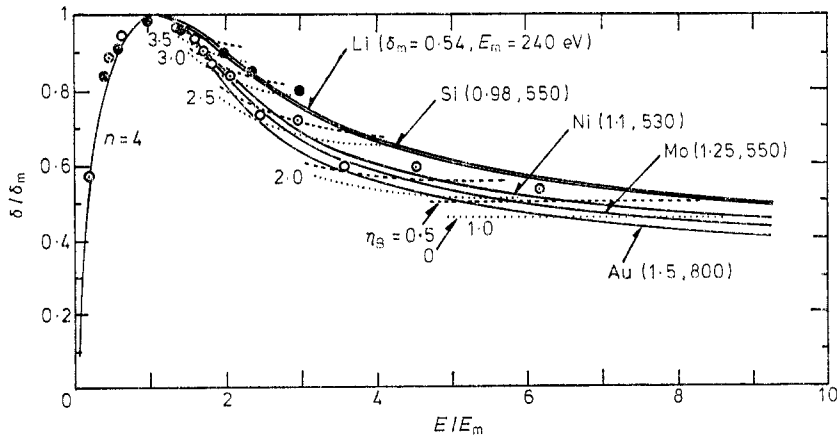

Figure 2. The theoretical and experimental comparison of the universal yield–energy curve for the energy-dependent parameter n. ● Si (Dionne 1975), ⊙ Ni (Knoll 1935), ○ Mo (Bruining 1942).

4. Quantitative characteristics of secondary yield

The value of the incident energy E_m for which the maximum yield occurs is related to α and c_0:

$$(E_m/E_R)^{1+1/n}=(c_0/\alpha)A_m=(c_0/\alpha)(1+5r^2) \tag{14}$$

where A_m is approximately given by equation (12) related with the back-scattering coefficient r. From equations (6) and (7), for the assumption $n=4$ in the first collision, which corresponds to the energy $E_m=500$–2000 eV, and the empirical data for Au: $E_m=800$ eV, $r=0{\cdot}45$, $I=9{\cdot}2$ eV, then the characteristic energy E_m is simply approximated as

$$E_m=57{\cdot}9Z^{1/15}I^{4/5}(1+5r^2)^{4/5}\ (\text{eV}). \tag{15}$$

On the other hand, the maximum yield δ_m is given by

$$\delta_m=\frac{K}{2}(c_0/\alpha)^{n/(1+n)}\,0{\cdot}365\,(1+1{\cdot}26\,r). \tag{16}$$

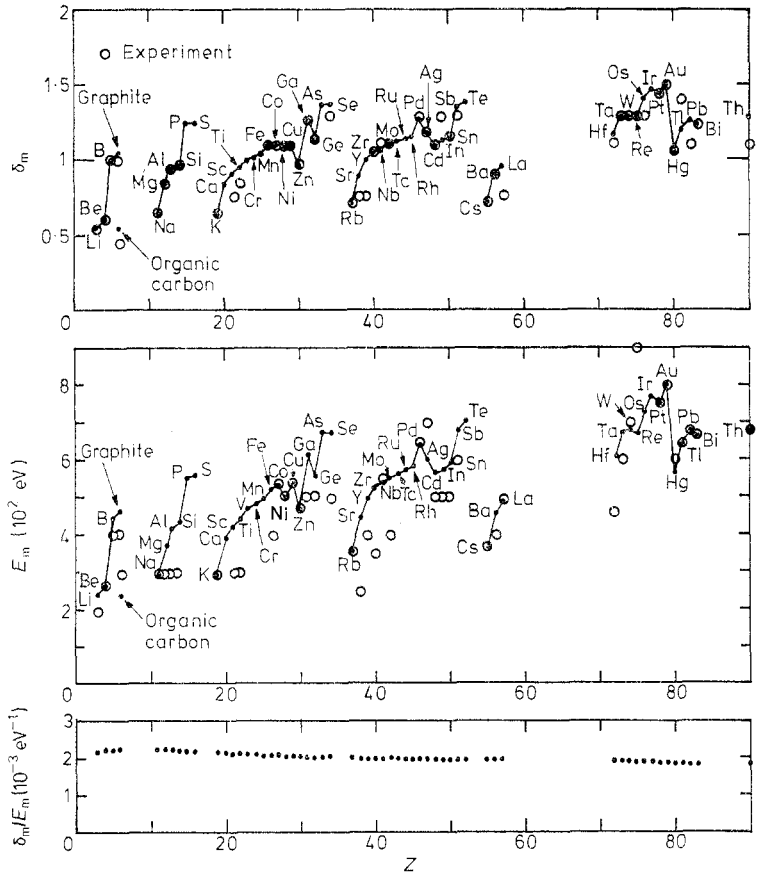

Figure 3. Comparison of the maximum yield of secondary electrons δ_m, the corresponding primary energy E_m and the ratio calculated by the range–energy retardation power formula with experiment.

According to the empirical relationship δ_m/E_m leads to

$$\frac{\delta_m}{E_m}=\left(\frac{K}{2}\right)\frac{0{\cdot}365\,(1+1{\cdot}26\,r)}{E_R\,(1+5\,r^2)^{4/5}}$$

$$\simeq K_0\,\frac{(1+1{\cdot}26\,r)}{(1+5\,r^2)^{4/5}} \tag{17}$$

where $K_0=2{\cdot}1\times10^{-3}$ (eV^{-1}) is closely fitted to $\delta_m=1{\cdot}5$ for Au.

Then, the maximum yield δ_m is empirically given by

$$\delta_m=0{\cdot}12\,Z^{1/15}\,I^{4/5}\,(1+1{\cdot}26\,r). \tag{18}$$

Figure 3 shows the above calculated results, compared with experimental results (Dekker 1958, Seiler 1967, Kollath 1956, von Ardenne 1956, Gobrecht and Speer 1953), in which experimental points are made to accord with calculated results when the differences are within 10%. The physical properties of materials used in calculation is shown in table 1, in which some of the data (as shown in parentheses) for the first ionisation

Table 1. Maximum yield and energy of secondary electrons, and atomic properties of target materials.

Atom	Z	I(eV)	r	E_m (eV) (expt)	δ_m (expt)	δ_m/E_m (10^{-3} eV^{-1})
Li	3	5·4	0·07	240 (100–200)	0·54 (0·47–0·55)	2·23
Be	4	6·0 (9·27)	0·08	270 (200–300)	0·61 (0·5–0·75)	2·24
B	5	10·9 (8·28)	0·08	450 (400)	1·0 (1·0)	2·24
Graphite	6	11·2	0·10	470 (300–400)	1·1 (0·9–1·0)	2·26
Organic C	6	4·9	0·10	240 (300)	0·55 (0·45)	2·27
Na	11	5·2	0·19	290 (300)	0·66 (0·65)	2·27
Mg	12	7·0 (7·61)	0·20	370 (300)	0·84 (0·8–0·9)	2·27
Al	13	8·0 (5·95)	0·20	420 (250–300)	0·95 (0·9–1·0)	2·26
Si	14	8·1	0·22	430 (300)	0·98 (0·9–1·1)	2·25
P	15	10·6	0·23	550	1·24	2·24
S	16	10·4	0·25	560	1·24	2·22
K	19	4·4	0·28	300 (300)	0·65 (0·55–0·69)	2·18
Ca	20	6·1	0·28	390	0·85	2·17
Sc	21	6·6	0·29	430 (300)	0·92 (0·75)	2·16
Ti	22	6·8	0·30	440 (300)	0·95 (0·75–0·85)	2·14
V	23	7·2	0·31	470	1·01	2·13
Cr	24	7·3	0·32	480	1·02	2·11
Mn	25	7·4	0·32	500	1·04	2·10
Fe	26	7·8	0·33	520 (400)	1·10 (1·1–1·32)	2·11
Co	27	7·8	0·33	530 (400–600)	1·10 (0·9–1·2)	2·08
Ni	28	7·6	0·34	530 (500–550)	1·10 (1·0–1·3)	2·07
Cu	29	7·7	0·34	530 (500–600)	1·11 (1·05–1·3)	2·08
Zn	30	6·5 (9·36)	0·35	470 (200–500)	0·97 (0·9–1·1)	2·06
Ga	31	9·0 (6·0)	0·35	610 (300–500)	1·27 (1·3)	2·07
Ge	32	7·9	0·35	560 (300–500)	1·15 (0·95–1·2)	2·06
As	33	9·8	0·36	670	1·37	2·04
Se	34	9·7	0·36	670 (400–500)	1·36 (0·6–1·3)	2·04
Rb	37	4·2	0·37	350 (350)	0·71 (0·7–0·85)	2·02
Sr	38	5·6	0·37	440 (250)	0·90 (0·75)	2·02

Table 1 (cont.)

Atom	Z	I(eV)	r	E_m (eV) (expt)	δ_m (expt)	δ_m/E_m (10^{-3} eV^{-1})
Y	39	6·4	0·38	500 (350–400)	1·00 (0·75)	2·00
Zr	40	6·8	0·38	530 (350)	1·06 (0·9–1·1)	2·02
Nb	41	6·9	0·38	540 (550)	1·07 (1·1–1·2)	1·99
Mo	42	7·1	0·38	550 (400)	1·10 (1·1–1·2)	2·00
Tc	43	7·2	0·39	560	1·12	1·99
Ru	44	7·4	0·39	580	1·15	2·00
Rh	45	7·4	0·39	580	1·15	1·98
Pd	46	8·3	0·39	640 (650)	1·27 (1·3)	1·99
Ag	47	7·6	0·39	600 (700)	1·18 (1·2–1·4)	1·97
Cd	48	7·0 (8·99)	0·40	560 (450–500)	1·11 (0·9–1·1)	1·97
In	49	7·1 (5·79)	0·40	570 (500)	1·13 (1·3–1·4)	1·98
Sn	50	7·3	0·40	590 (500)	1·16 (1·1–1·35)	1·97
Sb	51	8·7	0·40	680 (600)	1·34 (1·2–1·3)	1·97
Te	52	9·0	0·41	700	1·38	1·96
Cs	55	4·0	0·41	370 (300–400)	0·72 (0·5–0·76)	1·95
Ba	56	5·2	0·41	460 (400)	0·90 (0·65–0·9)	1·95
La	57	5·6	0·41	490 (500)	0·95 (0·80)	1·94
Hf	72	7·0	0·43	610 (460)	1·17 (1·1)	1·91
Ta	73	7·9	0·43	670 (600)	1·29 (1·1–1·35)	1·91
W	74	8·0	0·43	680 (700)	1·31 (1·05–1·4)	1·92
Re	75	7·9	0·43	680 (900)	1·29 (1·30)	1·91
Os	76	8·7	0·43	730	1·40 (1·30)	1·92
Ir	77	9·2	0·43	770	1·47	1·92
Pt	78	9·0	0·43	760 (700–750)	1·44 (1·35–1·7)	1·91
Au	79	9·2	0·45	800 (700–875)	1·50 (1·2–1·58)	1·88
Hg	80	6·0 (10·43)	0·45	570 (600)	1·06 (1·05)	1·86
Tl	81	7·0 (6·1)	0·45	640 (650)	1·21 (1·4)	1·88
Pb	82	7·5	0·45	680 (500–700)	1·27 (1·1)	1·86
Bi	83	7·3	0·45	670 (500–700)	1·25 (1·2)	1·87
Th	90	7·5	0·45	690 (600–800)	1·28 (1·1)	1·87

Physical data refer to *American Institute of Physics Handbook* (Dieke 1963, Frederikse 1963).

energy is corrected by the *Smithsonian Physical Tables* (1954) as follows; for B, Al, Ga, In, Tl the corrected value is the first ionisation energy plus 1–2 eV, but for He, Be, Mg, Zn, Cd, Hg the first ionisation energy minus 2–3 eV, and for the organic carbon the resonance potential of graphitised carbon is adopted.

For semiconductive compounds of the composition $(Z_1)_p(Z_2)_q$ in the similar treatment of Hohn and Niedrig (1972) it is assumed that the secondary yield of compounds is proportional to the atomic composition and the following relationships can be derived:

$$\delta_m = \frac{1}{p+q}(p\,\delta_{1m} + q\,\delta_{2m})$$

and

$$E_m = \frac{1}{p+q}(p\,E_{1m} + q\,E_{2m})\ (\text{eV})$$

where Z_1 and Z_2 are the atomic numbers of the constituent elements in the compound,

Table 2. Maximum yield and energy of secondary electrons of semiconductive compounds, and its atomic properties.

Material	I(eV)	r	E_m(eV)(expt)	δ_m (expt)	δ_m/E_m (10^{-3} eV^{-1})
Cu_2O	7·7 (Cu)	0·34 (Cu)	550	1·18	2·14
	13·6 (O)	0·15 (O)	(500)	(1·19–1·25)	
PbS	7·5 (Pb)	0·45 (Pb)	620	1·26	2·03
	10·4 (S)	0·25 (S)	(500)	(1·2)	
MoS_2	7·1 (Mo)	0·38 (Mo)	560	1·19	2·14
	10·4 (S)	0·25 (S)		(1·10)	
MoO_2	7·1 (Mo)	0·38 (Mo)	570	1·25	2·18
	13·6 (O)	0·15 (O)	(450)	(1·09–1·33)	
WS_2	8·0 (W)	0·43 (W)	600	1·26	2·10
	10·4 (S)	0·25 (S)		(0·96–1·04)	
Ag_2O	7·6 (Ag)	0·39 (Ag)	590	1·23	2·07
	13·6 (O)	0·15 (O)	(500)	(0·98–1·18)	

respectively. Table 2 shows the maximum yield and the primary energy of secondary electrons of semi-conductive compounds, compared with experiments, which are calculated by the above procedures.

5. Angular distribution of secondary electron emission

The angular distribution of the emitted electrons can be obtained by the aid of the calculation of §3. Let a part of the secondary electrons dislodged in a part of dx on the path of the primaries travel to the surface along the line l under an angle θ. To reach the surface the secondaries must travel a distance $l=x/\cos\theta$. Then, the secondary yield $\delta_p(\theta)$ due to primary electrons emerging in the direction l under an angle θ leads to

$$\delta_p(\theta)=(K/2)\int_0^R \left(\frac{dE/E_R}{dx}\right)\exp\left(\frac{\alpha x}{\cos\theta}\right)dx. \tag{19}$$

Then, $\delta_p(\theta)$, and $\delta_B(\theta)$ due to back-scattered electrons can be written as

$$\delta_p(\theta)=(K/2)\left(\frac{c_0}{\alpha\cos\theta}\right)^{n/(1+n)}\int_1^0 \frac{n}{1+n}(1-y)^{-1/(1+n)}A_\theta^{n/(1+n)}\exp(-A_\theta y)\,dy \tag{20}$$

$$\delta_B(\theta)=(K/2)\eta_B\left(\frac{c_0}{\alpha\cos\theta}\right)^{n/(1+n)}\int_{1/2}^0 \frac{2n}{1+n}(1-y)^{(n-1)/(n+1)}A_\theta^{n/(1+n)}\exp(-A_\theta y)\,dy \tag{21}$$

where

$$A_\theta=A/\cos\theta=(\alpha/c_0)(E_0/E_R)^{1+1/n}/\cos\theta.$$

6. Effect of incident angle to secondary yield

The calculation of $\delta(\nu)$ can be extended to the case where the primary beam strikes the surface under an angle ν to the normal. Secondary electrons dislodged at a point x on the path of the primary electrons in the material will then be located at a distance $x\cos\nu$ from the surface, so that in the above calculation x has to be replaced by $x\cos\nu$ and the absorption factor becomes $\exp(-\alpha x\cos\nu/\cos\theta)$.

If the new variable $A_\nu=(\alpha\cos(\nu)/c_0)(E_0/E_R)^{1+1/n}$ is substituted in equation (9),

$\delta(\nu)$ is given by

$$\delta(\nu)=(K/2)\left(\frac{c_0}{\alpha\cos\nu}\right)^{n/(1+n)}[f_{\mathrm{p}}(A_\nu)+\eta_{\mathrm{B}}f_{\mathrm{B}}(A_\nu)]. \tag{22}$$

Then, the secondary emission yield $\delta_{\mathrm{m}}(\nu)$ and its maximum $E_{\mathrm{m}}(\nu)$ normalised as a function of the incident angle ν of primary electrons become

$$\frac{\delta_{\mathrm{m}}(\nu)}{\delta_{\mathrm{m}}}=\frac{E_{\mathrm{m}}(\nu)}{E_{\mathrm{m}}}=(\cos\nu)^{-n/(1+n)}. \tag{23}$$

In scanning electron microscopes, as shown by Oatley *et al* (1965), an oblique illumination is very effective to collect secondary electrons satisfactorily, since too small secondary electron currents are subject to statistical quantum noise

7. Secondary electron emission yield transmitted

For a thin specimen with thickness d less than the penetration range R, the secondary electrons due to the electron beam bombardment on to the specimen are ejected from both surfaces, as has been recently investigated by Llacer (1968) and Jahrreiss (1972). The secondary electrons transmitted through the material follow the similar manner described in §3. Then, from equation (6) the transmitted secondary yield δ_{t} is given by

$$\delta_{\mathrm{t}}=(K/2)(c_0/\alpha)^{n/(1+n)}\int_0^{y_{\mathrm{d}}}\frac{n}{1+n}(1-y)^{-1/(1+n)}A^{n/(1+n)}\{\exp(-A(y_{\mathrm{d}}-y))$$
$$+A(y_{\mathrm{d}}-y)E_1[-A(y_{\mathrm{d}}-y)]\}\,\mathrm{d}y \tag{24}$$

where $y_{\mathrm{d}}=d/R$. And, moreover, the secondary yield δ_{s} from the surface of target for thin specimen with thickness d can be given by

$$\delta_{\mathrm{s}}=(K/2)(c_0/\alpha)^{n/(1+n)}\int_0^{y_{\mathrm{d}}}\frac{n}{1+n}(1-y)^{-1/(1+n)}A^{n/(1+n)}[\exp(-Ay)+AyE_1(-Ay)]\,\mathrm{d}y. \tag{25}$$

Figure 4 shows the comparison with the secondary yield δ_{t} and δ_{s} for the specimen thickness $d=50$ and 100 Å, where the parameters, n and c_0 given by equations (3) and (5), respectively, in the paper of Kanaya *et al* (1978) and as a function of A; $A=(\alpha/c_0)\times(E_0/E_{\mathrm{R}})^{1+1/n}$. It is found that both yields of δ_{t} and δ_{s} have maxima as a function of the incident energy depending on the penetration range and escape depth, which can be successfully interpreted by using A_{m} in equation (12). In the case of a gold target, for example, $A_{\mathrm{m}}=2$ calculated by equation (12) with $r=0{\cdot}45$ is in good agreement with the calculated ratio R/x_α $(=A_{\mathrm{m}}=\alpha R)=2$; for this target, $R=30$ Å and $x_\alpha=14$ Å at $E_{\mathrm{m}}=$ 800 eV. If the specimen for a scanning electron microscope (SEM) is thin enough and can be mounted to collect secondary electrons from both sides of the specimen surface, it may be a useful method for increasing the number of secondary electrons or for increasing the contrast of SEM images at the certain incident electron energy in which the maximum yield $(\delta_{\mathrm{t}}+\delta_{\mathrm{s}})$ occurs. As shown in the curves of δ_{s} for Au and Al targets, these theoretical curves δ_{s} are closely in agreement with experiments δ of Thomas and Pattinson (1970) for $E_0\leqslant 1{\cdot}5$ keV, and for $E_0>1{\cdot}5$ keV the experimental δ become larger than theoretical δ_{s} because the yields are dependent on the reduced depth, $y_{\mathrm{d}}=d/R$, of the film thickness d and the penetration range R in equation (24).

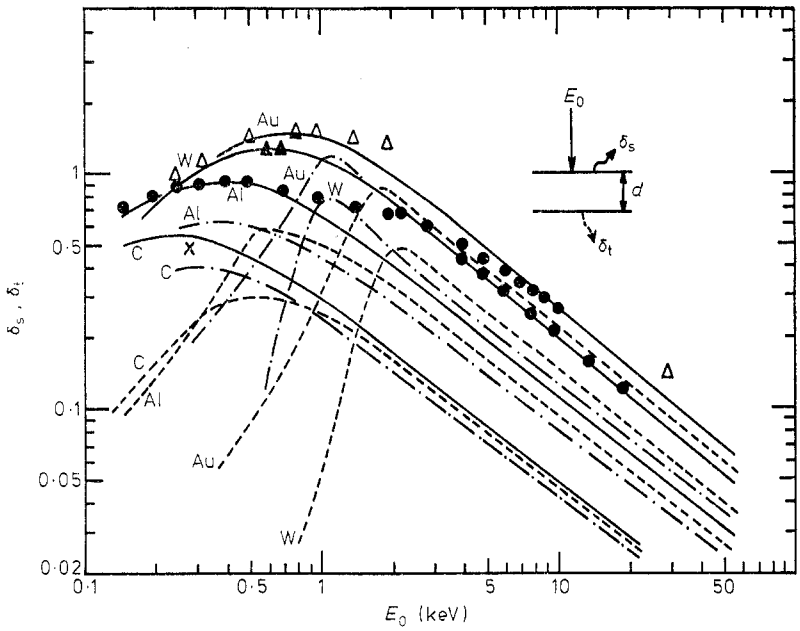

Figure 4. A comparison between the secondary yields δ_t and δ_s for the thicknesses $d=50$ and 100 Å. Experiments of δ for thick targets (△ Au; ▲ W; ● Al; × C, by Kollath 1956, Kanter 1961, Wittry 1966, Thomas and Pattinson 1970, Shimizu 1974) are plotted for a comparison with the theoretical curves of δ_t ($d=100$ Å). Calculated curves are drawn by ——— δ_s for $d=100$ Å, – – – – δ_t ($d=100$ Å), and —·— δ_t ($d=50$ Å). δ_s ($d=50$ Å) is smaller about 5–10% than the value of δ_s ($d=100$ Å) for $E_0 \leqslant 2$ keV. For $E_0 \geqslant 5$ keV the difference between δ_s ($d=100$ Å) and δ_s ($d=50$ Å) is very small.

8. Lateral distribution of secondary electron emission

The secondary electron yield $\delta(z)$ ejected from the surface at a distance z from the centre of the primary beam can be considered in similar manner. From the geometrical relation to the travelling distance l of secondary electrons given by

$$l=\alpha x/\cos\theta=\alpha Ry(1+\tan^2\theta)^{1/2}$$

with $\tan\theta=z/x$, the absorption term of secondaries can be derived as

$$\exp(-\alpha x/\cos\theta)=\exp[-\alpha R(y^2+(z/R)^2)^{1/2}]. \tag{26}$$

Accordingly, the secondary yields $\delta_p(z)$ and $\delta_B(z)$ due to primary and back-scattered electrons, respectively, are given by

$$\delta_p(z)=(K/2)(c_0/\alpha)^{n/(1+n)}\int_0^1\left(\frac{n}{1+n}\right)(1-y)^{-1/(1+n)}A^{n/(1+n)}$$
$$\times\exp\{-\alpha R[y^2+(z/R)^2]^{1/2}\}\,dy \tag{27}$$

$$\delta_B(z)=(K/2)\eta_B(c_0/\alpha)^{n/(1+n)}\int_0^{1/2}\left(\frac{2n}{1+n}\right)(1-y)^{(n-1)/(n+1)}A^{n/(1+n)}$$
$$\times\exp\{-\alpha R[y^2+(z/R)^2]^{1/2}\}\,dy. \tag{28}$$

Figures 5(*a*) and (*b*) show a comparison of the lateral distribution of secondary electrons $\delta(z)=\delta_P(z)+\delta_B(z)$ for Al and W targets, respectively, of thicknesses $d=50$ and 100 Å. These lateral distributions of the secondaries are important to determine the ultimate resolving power of the SEM. The distribution for Al target is broader than the distribution for a W target, in spite of the fact that r for Al is smaller than for W ($r=0{\cdot}2$ for Al and

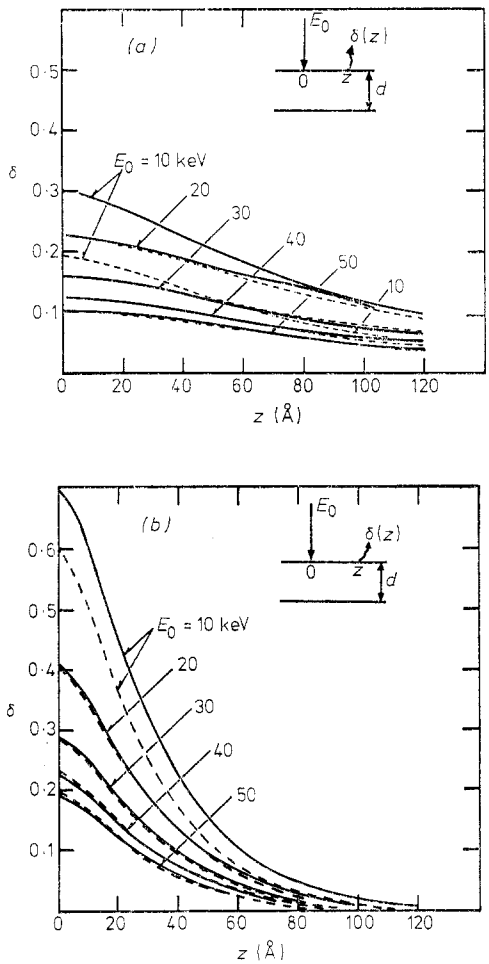

Figure 5. (*a*) The lateral distributions of secondary electrons for (*a*) Al and (*b*) W target for thicknesses $d=$(———) 100 and (– – –) 50 Å.

0·43 for W, respectively, calculated from Kanaya and Ono 1978), because the contribution of the back-scattered electrons for thin films may be very small. It is found that the contribution of the escape depth of secondaries is dominant for the sharp lateral distribution, and then we can expect sharp lateral distribution (higher resolution in SEM) when the escape depth of secondaries in the specimen is short. Moreover, it is shown that the yield of $\delta(z)$ for Al target in the thickness $d=50$ Å have a maximum yield at about 20 keV, relating with the film thickness and the escape depth of secondary electrons ($x_\alpha=38$ Å for Al).

9. Conclusions

(1) Based on the exponential power law for the screened atomic potential, secondary electron emission due to both primary and back-scattered electrons penetrating into metallic elements and semi-conductive compounds is developed in terms of the ionisation loss in the first collision for the escaping secondary electrons.
(2) The maximum yield and the corresponding primary energy can both consistently be derived as functions of three parameters: atomic number, first ionisation energy and back-scattering coefficient.
(3) The yield–energy curve as a function of the incident energy and the back-scattering coefficient are in good agreement with the experimental results.
(4) The energy dependence of the yield for thin films and the lateral distribution of secondary yield are derived as functions of the back-scattering coefficient and the primary energy.

References

Archard G P 1961 *J. Appl. Phys.* **32** 1505–9
von Ardenne 1956 *Tabellen der Elektronenphysik, Ionenphysik und Übermikroskopie* (Berlin: Springer) Nos 1, 2
Austin L and Starke H 1902 *Ann. Phys.* **9** 271–92
Baroody E M 1950 *Phys. Rev.* **78** 780–7
—— 1953 *Phys. Rev.* **89** 910
—— 1956 *Phys. Rev.* **101** 1679–84
Bruining H 1942 *Die Sekundär-Elektronen-Emission fester Körper.* (Berlin: Springer) p 60
—— 1954 *Physics and Applications of Secondary Electron Emission* (New York: McGraw-Hill) chap. 6
Cosslett V E and Thomas R N 1964 *Br. J. Appl. Phys.* **15** 1283–300
Dekker A J 1958 *Solid St. Phys.* **6** 251–311
Dekker A J and van der Ziel A 1952 *Phys. Rev.* **86** 755–60
Dieke G H 1963 *Am. Inst. Phys. Handb.* (New York: McGraw-Hill) §7 pp 14–5
Dionne G F 1973 *J. Appl. Phys.*, **44** 5361–4
—— 1975 *J. Appl. Phys.* **46** 3347–51
Frederikse H P R 1963 *Am. Inst. Phys. Handb.* (New York: McGraw-Hill) §9 pp 158–9
Fröhlich H 1932 *Ann. Physik.* **13** 229
Ganachaud J P 1977 *Thèse d'Etat*, Université de Nantes
Ganachaud J P and Cailler M 1975a *2e Colloq. Int. Phys. Cimie des Surfaces, Brest*
—— 1975b *Le Vide* **30A** 3
Glendenin L E 1948 *Nucleonics* **2** 12–32
Gobrecht H and Speer F 1953 *Zeit. Phys.* **135** 602
Hohn F J and Niedrig H 1972 *Proc. 5th Europ. Congr. on Electron Microscopy* pp 358–9
Holliday J E and Sternglass E J 1959 *J. Appl. Phys.* **30** 1428–31
Jahrreiss H 1972 *Thin Solid Films* **12** 187–200
Jonker J L H 1952 *Philips Res. Rept.* **7** 1–20
—— 1954 *Philips Res. Rept.* **9** 391–402
Kanaya K and Kawakatsu H 1972 *J. Phys. D: Appl. Phys.* **5** 1727–42
Kanaya K and Ono S 1976 *J. Phys. D: Appl. Phys.* **9** 161–74
—— 1978 *J. Phys. D: Appl. Phys.* **11** 1495–508
Kanaya K, Ono S and Ishigaki F 1978 *J. Phys. D: Appl. Phys.* **11** 2425–37
Kanter H 1961 *Phys. Rev.* **121** 677–80, 681–4
Katz L and Penfold A S 1952 *Rev. Mod. Phys.* **24** 28–44
Knoll M 1935 *Z. Tech. Phys.* **16** 467–75
Kollath R 1956 *Hdb. Phys.* (Berlin- Springer) **21** 232–303
Lane R O and Zaffarano D I 1954 *Phys. Rev.* **94** 960–4
Lenard P 1918 *Quantitatives uber Kathodenstrahlen aller Geschwindigkeiten* (Heidelberg: Carl Winter Universitatsbuchh)

Llacer J 1968 *SLAC Rept.* No. 86 (Stanford: Linear Accelerator Center)
Lye R G and Dekker A J 1957 *Phys. Rev.* **107** 977–81
Marshall J E 1952 *Phys. Rev.* **88** 416–7
Oatley C W, Nixon W C and Pease R F W 1965 *Adv. Electron. Electron Phys.* (New York: Academic Press) **21** 181–247
Pillon J and Ganachaud J P 1977 *Proc. 7th Int. Vac. Congr. Vienna* pp 473
Rauth A M and Simpson J A 1964 *Radiation Res.* **22** 643–61
Reimer L 1968 *Optik* **27** 86–98
Salow H 1940 *Z. Tech. Phys.* **21** 8
Seiler H 1967 *Z. angew. Phys.* **22** 249–63
Shimizu R 1974 *J. Appl. Phys.* **45** 2107–11
Shimizu R and Murata K 1971 *J. Appl. Phys* **42** 387–94
Smithsonian Physical Tables 1954 9th edn
Thomas S and Pattinson E B 1970 *J. Phys. D: Appl. Phys.* **3** 349–57
Weinryb E and Philibert J 1964 *C. R. Acad. Sci., Paris* **258** 4535–8
Wittry D B 1966 *X-ray Optics and Microanalysis* (Paris: Hermann) p 168
Wolff P A 1954 *Phys. Rev.* **95** 56–66
Wooldridge D E 1939 *Phys. Rev.* **56** 562–78
Young J R 1956 *J. Appl. Phys.* **27** 1–4
van der Ziel A 1953 *Phys. Rev.* **92** 35–9